

Flat and rounded contacts: Modelling the effect of a moment with application to fretting fatigue tests

J Strain Analysis
2023, Vol. 58(2) 91–97
© IMechE 2022



Article reuse guidelines:

sagepub.com/journals-permissions

DOI: 10.1177/03093247221089548

journals.sagepub.com/home/sdj



James PJ Truelove¹, David A Hills and Luke E Blades

Abstract

The problem of elastic indentation by a punch having the form of a flat front face but with edge rounding, and subject to both a normal load and moment, indenting an elastically similar half-plane is considered. Contact pressure in the neighbourhood of the edges shows a local peak, and the object of the paper is to show how different combinations of normal load and moment can give rise to the same near edge behaviour and peak pressure. The result found is very simple, and of direct practical application in fretting fatigue studies, both analytical and experimental.

Keywords

Fretting fatigue, contact mechanics, solid mechanics, experimental techniques, contact pressure

Date received: 17 December 2021; accepted: 2 March 2022

Introduction

The most common form of stationary contact we encounter in studies of fretting fatigue is one where the basic geometry of the contact-defining body has the form of a flat face with small radii at the ends. This is the basic shape of the dovetail root of a gas turbine fan blade and also the locking segments found in riser-wellhead connectors. Therefore, in order to obtain the best match of the behaviour of a contact under experimental conditions, that is also the form of the pad we use in laboratory fretting fatigue tests. There are four quantities which are important in defining the contact edge state of stress, including the effects of slip or localised plasticity: these are the normal load, P , and any moment present, M , together with the shear force supported by the contact, Q , and the presence of differential tensions acting parallel with the free surface. In the case of a Hertzian contact (which cannot support a moment) and other contact geometries which are very well represented by half-planes, certain combinations of material properties can result in the problem being uncoupled, such that the first two quantities define the normal problem and the contact pressure distribution while the second two excite shear and therefore encourage frictional slip.

Contacts having the ‘flat and rounded’ form, Figure 1, may not be particularly well modelled using half-plane theory if the contact extends a significant distance around the corner radius, so that the contact half-width, a , is

significantly greater than the flat contact length, b , but the limit $b/a \rightarrow 0$ implies a Hertzian contact which is represented well by half-planes. There has, so far, been no exhaustive examination of the limitations of the half-plane idealisation for these problems, although Davies¹ undertook a preliminary investigation. In fretting fatigue studies we are concerned primarily with the contact edges, which is where slip occurs and where cracks invariably nucleate, and the purpose of this paper is to undertake an investigation of near-edge conditions in the presence of a moment, and, in particular, to see how the moment modifies the local pressure distribution. Our motivation is to try to find how changes in normal load and moment interact, because we know that the prototypical problems experience a moment, but the test apparatus developed is not capable of applying an independent, controllable moment. On the other hand, in the test apparatus, because the shear force applied to the pad front face develops a moment within the projecting part of the pad, even if we contrive to react out the shear force in the plane of the contact a moment is still present, causing a small rotation and hence modification of the near-

University of Oxford, Oxford, UK

Corresponding author:

JPJ Truelove, Department of Engineering Science, University of Oxford, Parks Road, Oxford OX1 3PJ, UK.

Email: james.truelove@eng.ox.ac.uk

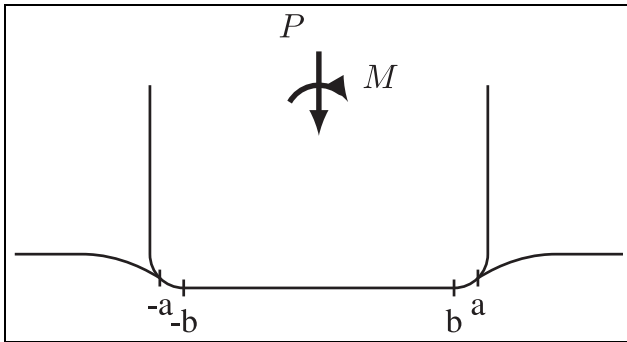


Figure 1. The geometry of a flat and rounded punch, as commonly used in fretting fatigue experiments.

edge pressure distribution. This moment has been shown² to be proportional to the shear force, and the constant of proportionality between the two seems to be essentially a property of the test apparatus, and to depend only very weakly on normal load. In Truelove et al.² we showed how the normal load might be varied so as to compensate for this effect, but the procedure used was ad hoc and based on a rather complex half plane solution for a three part punch,³ and so here we aim to set out a simple, closed form alternative.

Domain shape of the contact edge

Before we develop the theory itself it will be helpful to look in some detail at the nature of the contact edge and its characteristic form, and in this sense this is a development of the argument made at the beginning of the last paragraph. The geometry under consideration is shown in Figure 2, which shows a close up of the edge of the contact in Figure 1. For simplicity we will assume that the bodies forming the contact have the same elastic properties, with Young’s modulus E and Poisson’s ratio ν .

If, first, we zoom very close in to the extreme edge of the contact, each body clearly behaves like a half-plane, and therefore, if we take a coordinate s from the contact edge the contact pressure will vary in the form

$$p(s) = L_I \sqrt{s} \tag{1}$$

where L_I is a constant which may, in principle, be found for any specific contact geometry.^{4,5}

What we would like to do is to establish an asymptotic form which extends further out from the contact edge but, to do so we should, as a precursor, look at the characteristic form of the solution anticipated when $s \gg a - b$, although not so large that the solution ‘feels’ the presence of the opposite end of the contact. Refer, again, to Figure 2, but now look at what we might anticipate at remote points. The presence of the rounding will become increasingly irrelevant, and the characteristic solution will be governed by the effects of the half plane free surface together with the free straight surface – here shown as normal to the half-plane, but note that there are other possibilities. If, away from the contact edge the

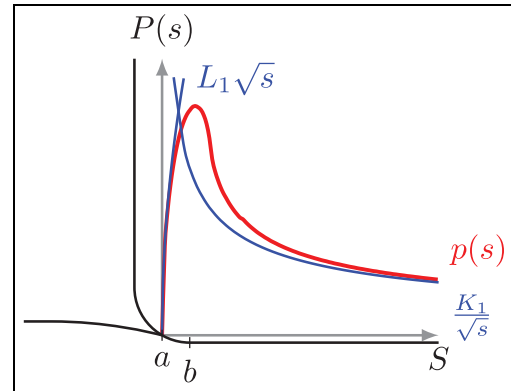


Figure 2. The geometry of the corner of the flat and rounded punch, showing the stress asymptotes.

interface is stuck, the relevant domain shape becomes one of a monolithic wedge whose internal angle is the sum of the half-plane plus the contact-defining body, and so, for the problem illustrated, and also for the pads used in the test apparatus, this is a three quarter plane. The Williams solution⁶ shows us that the contact pressure and, indeed, all components of stress within the pair of bodies must decay in a power order manner given by

$$\sigma_{ij}(r, \theta) = K_I r^{\lambda_I - 1} f_{ij}^I(\theta) \tag{2}$$

where $\lambda_I = 0.5445$, and the eigenvector $f_{ij}^I(\theta)$ is fully specified. Guided by these results Fleury et al.^{4,5} developed a characteristic solution for a rounded quarter plane in partial slip contact with an elastically similar half-plane. One of the principal outcomes of that piece of work was the pressure distribution at the contact edge, and it was shown⁷ that this solution could convincingly be used to introduce the effects of rounding to a sharp cornered contact. Although it was never extended to the effects of a moment, that could certainly also be done. But, although this solution is attractive because it is mathematically rigorous, the difficulty in employing it stems from the fact that the first, symmetric, solution (quoted above) and the second term in the series, which is antisymmetric, uncouple along the bisector line, and this means that it is very complicated indeed to make use of in the context of the contact problem because the normal loads and shear loads both excite both eigensolutions.

An earlier attempt to solve the same problem used the half-plane result for the contact pressure distribution induced by the finite flat and rounded punch^{8,9} using uncoupled half-plane theory, taking the limit where, separately, $a, b \rightarrow \infty$, but where $a - b$ remains finite.¹⁰ When the limit stated is taken, we find that the contact pressure distribution takes the following form

$$\frac{2\pi R}{E^*} p(s) = 2\sqrt{ds} + (s - d) \ln \left| \frac{\sqrt{d} - \sqrt{s}}{\sqrt{d} + \sqrt{s}} \right| \tag{3}$$

where $d = a - b$ and R is the radius of the corner rounding. When $s \gg d$ this reduces to the form

$$p(s) = \frac{K_I}{\sqrt{s}} \quad (4)$$

where the asymptotic equivalent of the contact law is

$$\frac{2\pi R}{E^*} = \frac{4\sqrt{d^3}}{3K_I} \quad (5)$$

and hence

$$p(s) = \frac{3K_I}{4\sqrt{d^3}} \left[2\sqrt{ds} + (s-d) \ln \left| \frac{\sqrt{d} - \sqrt{s}}{\sqrt{d} + \sqrt{s}} \right| \right] \quad (6)$$

Very close to the contact edge, where $s \ll d$ the stress contact pressure will be square root bounded, with form given by equation (1) with

$$L_I \equiv \frac{3K_I}{d}. \quad (7)$$

This is a very attractive, clean, tidy solution *but* it incorporates the result that when the observation point is very remote from the contact edge the pressure decays in a square root manner, equation (4), whereas we expect, from our observations in the last paragraph that it *ought* to decay in the form $p(s) \sim s^{-0.45}$. It is this result which highlights the other possible way, as an alternative to elastically similar bodies, in which the requirement that Dundurs' second constant may be made to vanish. Specifically, if $E_1 \rightarrow \infty$ (the contact-defining body becomes rigid) whilst $\nu_2 \rightarrow 1/2$, that is, the half plane becomes incompressible.

Other properties of the solution may be found. For example, the maximum value of the contact pressure, that is, the peak in Figure 2, is given by

$$p_{max} = 1.074 \left(\frac{K_I^2 E^*}{R} \right)^{1/3}. \quad (8)$$

Sharp edged punch approximation

If the edge radius of the contact-defining body is small compared with the contact half width the geometry of the punch may be approximated by a simple square-ended form, and when this pressed into contact with an elastic half plane by a normal force and clockwise moment the stress intensity factor at the left hand edge is given by.¹¹

$$K_I = \frac{1}{\pi\sqrt{b}} \left[P - \frac{2M}{b} \right] \quad (9)$$

where K_I is related to the near edge contact pressure by equation (4). It follows directly that, in any two problems, provided the value of this quantity is the same at a contact edge the local contact pressure and attendant stress field will be the same, that is, if we have two contacts 1 and 2 local pressure will be maintained at the same value provided only that they are made from the same material and have the same edge radius, if

$$P_1 - \frac{2M_1}{b} = P_2 - \frac{2M_2}{b}. \quad (10)$$

Example results and comparisons

We will consider now how well the method derived applies to contacts found in practical problems, and the range of loads and geometries over which the solution could be thought of as valid. The semi-infinite solution cannot sense whether the load it is subjected to arises from a normal load or a moment, so in order to see how well the solution applies to a real punch geometry the contact pressure distribution for a finite flat and rounded punch is required. The solution derived by Andresen et al.³ was used, the contact pressure being given by:

$$p(x) = - \frac{\sqrt{(a+x)(c-x)}}{A\pi R} * \left[\frac{(b+x) \log \left(\left| \frac{(a+c)(b+x)}{(c-a)(x-b) + 2(ac+bx) + 2\sqrt{(a-b)(b+c)(c-x)(a+x)}} \right| \right)}{\sqrt{(a+x)(c-x)}} + \frac{(b-x) \log \left(\left| \frac{(a+c)(b-x)}{(c-a)(b+x) + 2(ac-bx) + 2\sqrt{(a+b)(c-b)(c-x)(a+x)}} \right| \right)}{\sqrt{(a+x)(c-x)}} + \cos^{-1} \left(\frac{-a+2b+c}{a+c} \right) + \cos^{-1} \left(\frac{a+2b-c}{a+c} \right) \right] \quad (11)$$

Where a and c , the locations of the edge of the contact are found using an iterative solver and the side

conditions for normal (equation (12)) and rotational (equation (13)) equilibrium,

$$\frac{4PA}{(a+c)^2} = - \left(-\frac{\sqrt{(a-b)(b+c)}(-a+2b+c)}{R(a+c)^2} + \frac{\cos^{-1}\left(\frac{-a+2b+c}{a+c}\right)}{2R} - \frac{\sqrt{(a+b)(c-b)}(a+2b-c)}{R(a+c)^2} + \frac{\cos^{-1}\left(\frac{a+2b-c}{a+c}\right)}{2R} \right) \quad (12)$$

$$\frac{4PAs}{(a+c)^2} = (a-c)* \left(\frac{\sqrt{(a-b)(b+c)}\left(\frac{a^2-2b^2+c^2}{a-c} + \frac{1}{2}(a-2b-c)\right)}{3R(a+c)^2} - \frac{\sqrt{(a+b)(c-b)}\left(\frac{a^2-2b^2+c^2}{a-c} + \frac{1}{2}(a+2b-c)\right)}{3R(a+c)^2} + \frac{\cos^{-1}\left(\frac{-a+2b+c}{a+c}\right)}{4R} + \frac{\cos^{-1}\left(\frac{a+2b-c}{a+c}\right)}{4R} \right) \quad (13)$$

where s is the eccentricity of the normal load (such that $Ps = M$) and A is given by $A = \frac{4(1-\nu^2)}{E}$ under conditions of plane strain.

The inputs to the problem can be arranged into three dimensionless groups, $\frac{M}{Pb}$, $\frac{R}{b}$ and $\frac{K_I}{E*\sqrt{b}}$, one of which defines the geometry of the punch, and two of which define the applied loading. The output contact pressure distribution is normalised by $\frac{K_I}{\sqrt{b}}$, which simply represents the combined magnitude of the moment and normal load.

It is worth noting that equation (9) sets an upper limit on the largest possible value of $\frac{M}{Pb}$. At the right hand edge of the contact separation will occur when the value of K_I becomes negative, which occurs when $\frac{M}{Pb} = \frac{1}{2}$.

Figure 3 shows the contact pressure distribution for a number of moment-normal force loading mixtures, chosen through the use of equation (9) such that they

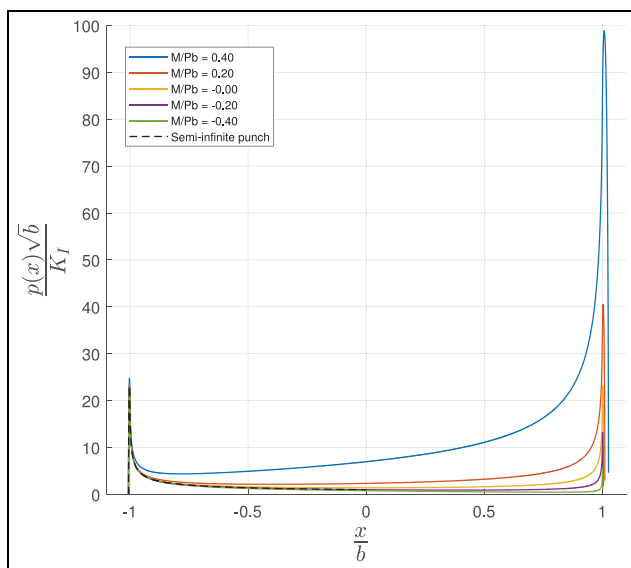


Figure 3. A plot of the contact pressures across the entire contact for various values of $\frac{M}{Pb}$, for $\frac{R}{b} = 0.1$, $\frac{K_I}{E*\sqrt{b}} = 0.001$.

have equivalent values of K_I at the left hand edge of the contact. In this plot the values chosen represent a punch having a geometry defined by $\frac{R}{b} = 0.1$, applied loading of $\frac{K_I}{E*\sqrt{b}} = 0.001$ and various values of loading mixture, $\frac{M}{Pb}$, from 0.4 to -0.4 , values which roughly correlate with those that may be found in a typical fretting fatigue test. The figure illustrates clearly the effect of matching moment-normal load pairs: at the left hand edge of the contact the local contact pressure distributions are almost identical; at the right hand edge they diverge drastically. Note that, although at this scale the contact pressure appears to be singular in character at the peaks in the distribution, these are, in fact, rounded.

Figure 4 shows the detail of the leftmost edge of the contact pressure distribution, allowing closer inspection

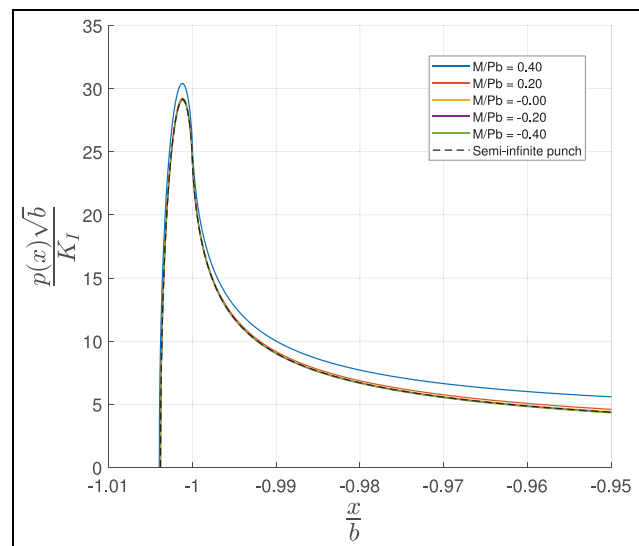


Figure 4. A plot of the contact pressures at the left hand edge of the contact, over a sweep of values of $\frac{M}{Pb}$, for $\frac{R}{b} = 0.1$, $\frac{K_I}{E*\sqrt{b}} = 0.001$.

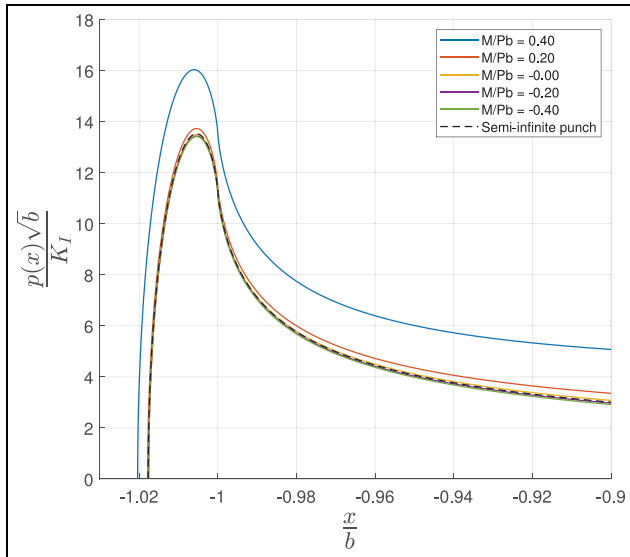


Figure 5. A further example of matching equivalent pairs of P-M loadings, in this plot for the case $\frac{R}{b} = 1$, $\frac{K_I}{E^*\sqrt{b}} = 0.0005$.

of the localised contact pressure in the region surrounding the corner rounding. As in Figure 3 the various solid coloured lines are solutions from the finite width punch contact pressure distribution (equation (11)), the dashed line represents the semi-infinite flat and rounded punch approximation (equation (6)). It can be seen that for the majority of load cases the solutions lie extremely close together, with the plots only starting to diverge at large values of positive moment, due to the left hand edge of the contact sensing the effect of the increased contact pressure at the right hand side of the contact (with the sense of the moment being as drawn in Figure 1, such that a positive value of moment causes an increase in contact pressure at the right hand edge of the contact).

Another example of the accuracy of the moment matching achievable is shown in Figure 5, This time for the rather geometrically extreme case $\frac{b}{R} = 1$. We would intuitively not expect the method described to be valid in this regime as the assumption that the amount of corner rounding is small compared to the half width of the punch is evidently not valid, but as shown in Figure 5 the method holds reasonably well, even under these conditions. The deviation with the application of large positive moments is greater than in the previous plot, as the reduced distance between the edges of the contact means that they influence each other to a greater degree.

It would seem a natural next step would be to attempt to quantify the difference between the theoretical semi-infinite pressure distribution and the pressure distribution for a finite width punch over a range of loading conditions and geometries. Figure 6 shows the results of one method of attempting to measure this change. One way of characterising the near edge stress field of an incomplete contact is through the use of a

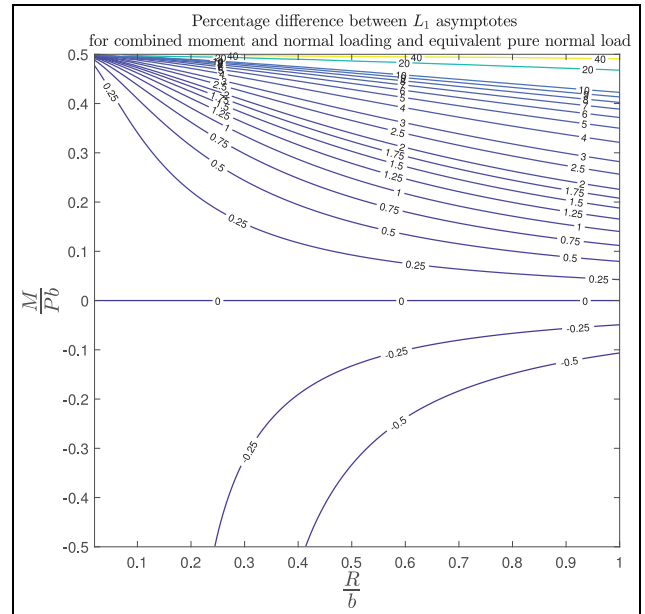


Figure 6. The percentage difference in the outer L_1 asymptotes comparing the moment and normal load problem to the equivalent normal load problem calculated using the method derived in this paper.

square root bounded asymptotic multiplier, L_I . In Figure 6 the value of P is held constant at a value of 1000 N/mm, with corner radius fixed at 1 mm and steel like material properties, while the applied moment and contact flat width are varied. For each load/geometry combination the value of L_I is calculated for two load cases, the combination of moment and normal load indicated on the chart, and an equivalent pure normal load, found using equation (10). The percentage difference between these two values of L_I is calculated, naturally the better our model the closer we would expect the values of L_I to be and therefore the closer the equivalent stress fields. Since one of the primary assumptions we have made in this model is that the two ends of the contact are uncoupled and can be analysed independently we would expect good results when there is either significant geometric separation between the two ends of the contact ($b > R$) or when the loads are low enough to prevent the peaks in contact pressure from interfering. The contour plot shows that the method found in this paper achieves a good level of agreement across a large range of loads and geometries, with even fairly severe load and geometry combinations producing single digit percentage differences.

Application to fretting fatigue experiments

An obvious application of this method is to the study of the effects of moments in fretting fatigue experiments. Figure 7 shows an example of a typical test rig used in Oxford for the study of fretting fatigue problems, and

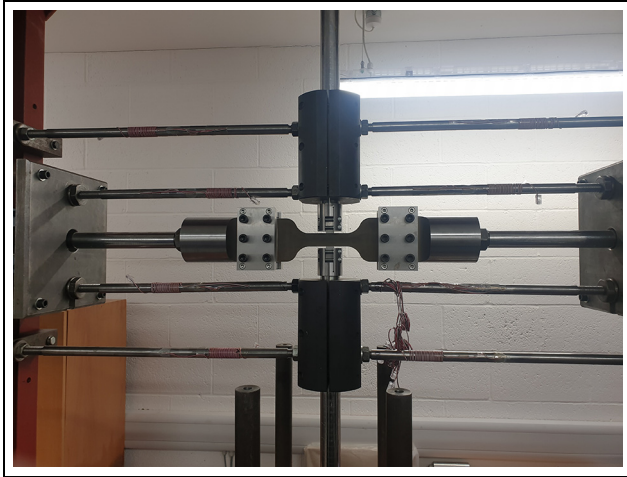


Figure 7. An image of the fort rig, a typical piece of test apparatus used in the study of fretting fatigue phenomenon.

illustrates the typical layout of actuators. A pair of pads bear on a dogbone specimen, a hydraulic actuator at the base of the rig providing normal load. A further pair of actuators to the left and right of the specimen apply loads to it, so through the application of differential loads to each end of the specimen shear loading can be applied. The rig as built has no facilities to apply moments: only the normal load, shear load and bulk tension are controllable, but if a procedure such as the one derived in this paper is used it becomes unnecessary to be able to control the moment directly. Generally there are a couple of situations in which we may wish to account for the presence of a moment in an experiment:

- The study of contacts where the prototype component is loaded with large moments
- To account for the effects of moment coupling phenomenon arising from the design of the apparatus²

As an illustrative example let us briefly consider a problem of the second kind.

As described in Truelove et al.,² moment coupling is the generation of an undesired moment across a contact during a fretting fatigue experiment. These moments can arise from a number of sources, including deformation of the test apparatus, and the fact that it is impossible to construct a practical pad with true half plane geometry – the pad must include some form of projection which then deforms as a stubby cantilever under the application of shear load. For the fort rig illustrated in Figure 7 the load paths through the rig are a major source of coupled moments, in that the shear load is supported through leaf springs at a significant distance from the contact.

First, the coupling coefficient between the applied shear force on the pair of pads, Q , and the moment present must be found. One possibility we have

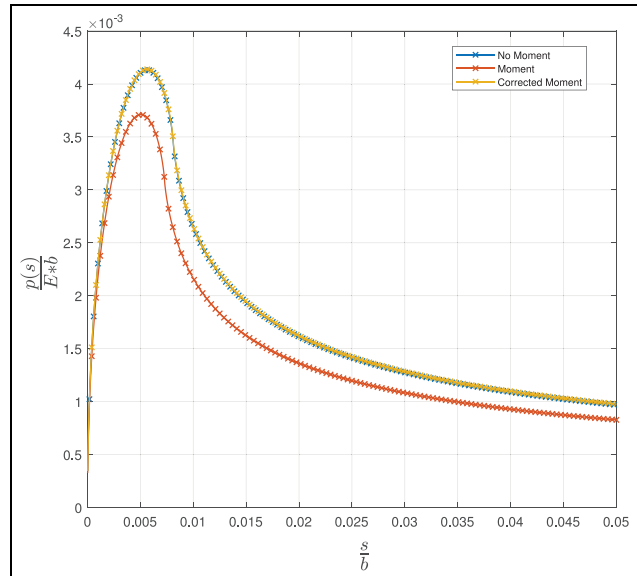


Figure 8. A three way comparison between the pressure distribution for a punch with no moment, a punch with a moment applied and a punch with normal load varied in a way such that the effect of the moment is cancelled out.

successfully used is an optical lever across the width of laboratory, digital image correlation has also been used successfully. This provides k where

$$M = kQ \quad (14)$$

Therefore, through equation (9), if the prototype experiences a load set $(P_p, Q_p, M_p, \sigma_p)$ the loads which must be applied on the test apparatus, P_T , is given by

$$P_T = P_p - \frac{2(M_p - kQ_p)}{b_T}, \quad (15)$$

where b_T is the half-width of contact in the laboratory test.

As an example consider Figure 8. This represents a case where we wish to run an experiment on a rig with a known amount of moment coupling, but where we would like to run the test under conditions equivalent to a constant normal force loading, that is, the near edge contact pressure should remain constant throughout the loading cycles. The plot shows three lines; in blue we have the idealised pressure distribution without any moment, whereas in orange we have the pressure distribution that would actually occur at the point in the load cycle where maximum moment occurs, which corresponds to the point of maximum applied shear. Through the use of equation (15) with $M_p = 0$ it is possible to write down the equivalent value of P which will allow us to recover the same contact pressure distribution as the no moment case, shown in Figure 8 in

yellow. It can be seen that the blue and yellow pressure distributions are almost coincident, and so the effect of a moment has been removed on a test rig that does not have moment control. Using this procedure the contact pressure has only been matched at one edge of the contact, however, in most fretting fatigue experiments where a combination of shear and bulk load one end of the pad will be more highly loaded. As such we can predict which end of the pad will experience failure, and therefore we know end of the pad we should control the contact pressure at before the test is started.

Conclusion

In this paper we have described a method of modelling the effect of an applied moment to a flat and rounded punch by adding a local solution for corner rounding to a solution for a sharp ended punch. It was demonstrated that the sharp punch and rounding model approximated a finite flat and rounded punch solution over a range of contact geometries. The solution for a sharp edged punch was therefore used to find a way of connecting equivalent P, M pairs for flat and rounded contacts, and it is shown that this model applies over a wide range of punch geometries and load cases.

In the formulation used here the finite punch solution is an elastically similar elastic-elastic problem, whereas the square edged punch formulation uses a rigid punch on an incompressible half plane. Both these formulations result in Dundur's second parameter being equal to zero, so that the normal and tangential problems are uncoupled and the application of normal loading does not generate shear tractions across the contact interface.

The method outlined in this paper has practical application to fretting fatigue experiments, allowing for both the addition and removal of equivalent moments from experiments while using rigs that do not have facilities to control moment loading.

Declaration of conflicting interests


The author(s) declared no potential conflicts of interest with respect to the research, authorship, and/or publication of this article.

Funding

The author(s) disclosed receipt of the following financial support for the research, authorship, and/or publication of this

article: James Truelove acknowledges with thanks the award of an iCASE award ref 17000027 from Rolls-Royce plc which has enabled him to carry out this work. David Hills and Luke Blades acknowledge Rolls-Royce plc and the EPSRC for their support under the Prosperity Partnership Grant: 'Cornerstone: Mechanical Engineering Science to Enable Aero Propulsion Futures', Grant Ref: EP/R004951/1.

ORCID iD

JPJ Truelove  <https://orcid.org/0000-0001-6354-3908>

References

1. Davies M. *Studies in contact mechanics with reference to fretting fatigue of gas turbine blade/disc attachments*. D.Phil Thesis, University of Oxford, UK, 2012.
2. Truelove J, Hills DA and Blades LE. Measurement of moment coupling in fretting fatigue experiments. *Proc IMechE, Part C: J Mechanical Engineering Science* 2021; 235(24): 7726–7733.
3. Andresen H, Hills DA and Vázquez J. Closed-form solutions for tilted three-part piecewise-quadratic half-plane contacts. *Int J Mech Sci* 2019; 150: 127–134.
4. Fleury RMN, Hills DA and Barber JR. A corrective solution for finding the effects of edge-rounding on complete contact between elastically similar bodies. Part I: contact law and normal contact considerations. *Int J Solids Struct* 2016; 85–86: 89–96.
5. Fleury RMN, Hills DA and Barber JR. A corrective solution for finding the effects of edge-rounding on complete contact between elastically similar bodies. Part II: near-edge asymptotes and the effect of shear. *Int J Solids Struct* 2016; 85–86: 97–104.
6. Williams ML. Stress singularities resulting from various boundary conditions in angular corners of plates in extension. *J Appl Mech* 1952; 19: 526–528.
7. Hills DA, Ramesh R, Fleury RMN, et al. A unified approach for representing fretting and damage at the edges of incomplete and receding contacts. *Tribol Int* 2017; 108: 16–22.
8. Ciavarella M, Hills DA and Monno G. The influence of rounded edges on indentation by a flat punch. *Proc IMechE, Part C: J Mechanical Engineering Science* 1998; 212(4): 319–327.
9. Steuerman I. *Contact problem of the theory of elasticity*. Moscow: Gostekhizdat, 1949.
10. Sackfield A, Mugadu A, Barber JR, et al. The application of asymptotic solutions to characterising the process zone in almost complete frictionless contacts. *J Mech Phys Solids* 2003; 51: 1333–1346.
11. Sackfield A, Truman CE and Hills DA. The tilted punch under normal and shear load (with application to fretting tests). *Int J Mech Sci* 2000; 43: 1881–1892.